Autonomous Light-Weight Heliostat With Rim Drives

Andreas Pfahl[1], **Michael Randt**[2], **Stephan Kubisch**[2], **Carsten Holze**[3], **Helmut Brüggen**[3]

[1] German Aerospace Centre (DLR), Institute of Solar Research, Pfaffenwaldring 38-40, 70569 Stuttgart, Germany,

Phone: +49-7116862479, Fax: +49-71168628032, E-mail: Andreas.Pfahl@dlr.de

[2] TRINAMIC Motion Control GmbH & Co KG, Waterloohain 5, 22769 Hamburg, Germany

[3] toughTrough GmbH, Fahrenheitstrasse 1, 28359 Bremen, Germany

Abstract

To achieve the current challenging cost objectives, several approaches for cost reduction, which fit well to each other, are combined: The wind loads are reduced by appropriate manipulators which reduces weight and cost of the heliostat structure and the ground anchor foundation. Laminated mirror facets are of high reflectivity and shape accuracy and of low weight. The low weight is advantageous for the dimensioning of the bearings and regarding energy consumption. Energy consumption is further reduced by a highly efficient drive train. Thus small capacity of the wireless energy supply of the autonomous heliostat is sufficient which reduces significantly its cost. By the combination of horizontal primary axis with rims and winch wheels a cheap and precise solution for the drives was found. Ray tracing calculations show that the losses due to the reduced angle range are negligible. With the new heliostat concept the current cost goals seem to be achievable.

Keywords: central receiver, wind load reduction, autonomous heliostat, rim drives, sandwich facet, ground anchor foundation

1. Introduction

Heliostats are the most important cost element of power tower plants because they typically contribute about 50% to the total cost of the plants [1]. Therefore, in particular the cost of heliostats must be reduced to reach the current challenging cost objectives. To achieve 10 ¢/kWh by solar thermal tower power plants, the heliostat field may cost 120 \$/m², to reach 6 ¢/kWh it may cost 75 \$/m² [2]. With the conventional heliostat concepts this is hardly achievable. Beneficially an impressive amount of unconventional heliostat concepts was found so far as surveyed in [3]. From these concepts and with the knowledge about wind loads [4] and their impact on the annual energy yield [5], a new combination was found which leads to a significant cost reduction. It combines the advantages of the following approaches: sandwich mirror facets [6], wind load reduction [7], prefabricated compact ground anchor foundation, wireless communication and energy supply [8], horizontal primary axis [9], rim drives [10] with winch wheels and locking during stow [3] (Fig. 1). In the following, the wind load assumptions, the mechanical structure, the drives and the control of the new heliostat concept is described and rough cost estimation for a heliostat of 8m² is given.

Fig. 1. Autonomous light-weight heliostat with rim drives

2. Wind loading and manipulators for their reduction

Fundamental design criteria for heliostats are mostly depending on the site relevant environmental conditions. Usually the systems will face flat land scape with corresponding high wind loading (average and peak loading) and wind driven sand loading, causing abrasion, especially in desert regions.

Basic design criteria for the systems are:

- minimum deformation/slope error due to self-weight effects and additional wind loading for the mirror surface in operation conditions to guarantee maximum system efficiency and
- survival of all heliostat system components (mirror facets-, supporting structure, drives and pylon) at maximal wind loading in stow position.

Both design criteria have to be combined to realize optimized structural designs and light weight configurations.

The general wind loading conditions for the design of heliostat systems are given by accordant standards, for example EC 1 [11]. Structural forces and corresponding torque moments can be determined for the relevant operation conditions and the stow position. Numerous experimental studies have been performed in the past to get more accurate design relevant data for isolated heliostat, as well as for complete heliostat field configurations (e.g. [12],[13] and [4]). The detailed studies of distinguished configurations are the current base for the dimensioning of heliostats. At these the turbulence intensity is matched, but not the turbulence spectrum. David Banks [14] pointed out that without matching the turbulence spectrum the wind loads are presumably overestimated especially in the stow position. This question has to be further investigated and may lead to a reduction of the load assumptions and therefore to lower cost.

Furthermore, parametric wind tunnel investigations of generic heliostat configurations showed high potential for load decrease up to 50% by manipulators; results can be found at [7]. By optimization of the heliostat itself, due to the integration of manipulators and in combination with the overall heliostat field layout, even higher reduction of structural and torque loads for the relevant operation conditions have been proven. The manipulators may consist of porous "fences" around the mirror facet. Their impact on the wind loads have been investigated by wind tunnel measurements (Fig. 2).
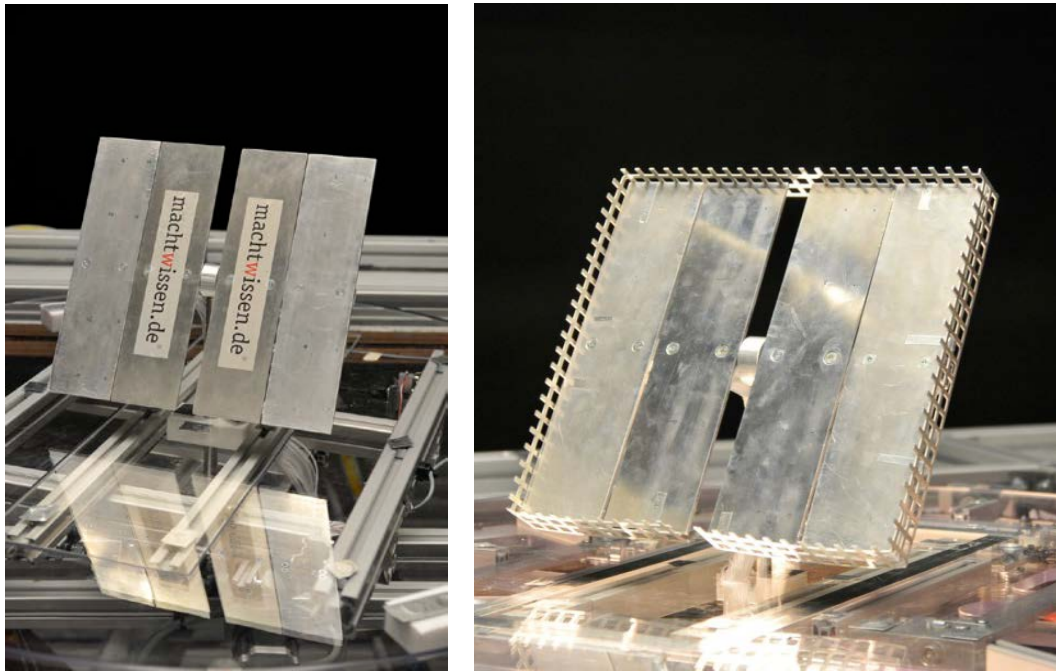
Fig. 2. Left: Isolated heliostat model, mounted on six component balance in wind tunnel. Right: heliostat with edge manipulator (academic test case)

For the dimensioning of heliostats the overturning moment during storm conditions is decisive. As wind in the atmospheric boundary layer is not laminar but turbulent, the frontal edge is instantaneously attacked also normal to the mirror plane. The sideward flow separates at the frontal edge, causing suction on the other side of the mirror, which leads to high pressure coefficients near the frontal edge [15], and causes high peak overturning moment (Fig. 3 left). By manipulators (porous "fences" at the edges) separation and thus suction is reduced which leads to a significant reduction of the overturning moment (Fig. 3 right).
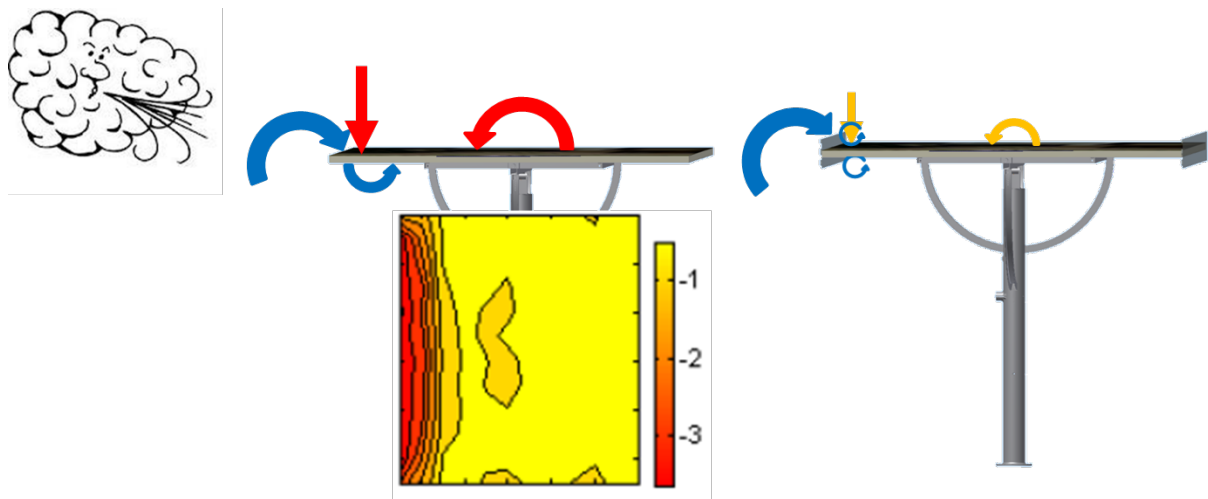
Fig. 3. Left: Turbulences causing high pressure coefficients at the frontal edge [15] and high overturning moment at storm conditions with heliostat in stow position. Right: Manipulators reducing suction and overturning moment

The cross-sectional area of tubes or I-beams is proportional to the load moment to the power of 2/3 ([1] A.3). Assuming a load reduction of about 40%, the weight of components, for which the dimensioning depends on this load, could theoretically be reduced by about 30%. Such components are the structural support with bearings, the pylon, the foundation and partly the mirror facet.

3. Sandwich facet

Based on the structural loads, a sandwich mirror facet, consisting of a thin glass mirror as front layer, a standard foam core and a steel backward layer (Fig. 4), has been optimized. The facets can be manufactured as plain mirrors for mechanical bending in an integrated frame or shaped in three dimensions by a precision molding process. Due to the high self-stiffness of the sandwich itself, no additional stiffeners are needed. The specific structural weight of the mirror facet, including the mechanical interfaces, is below 10kg/m².

Fig. 4. Laminated mirror facets for heliostats

Assuming cost of 12$/m² for 0.5mm steel back layer, also about 12$/m² for thin glass mirrors (compare [1]) and 15$/m² for core and assembly, about 40$/m² for the sandwich facet result (for high production rate). Due to the higher reflectivity of thin glass mirrors of about 2% and lower slope error of measured 0.6mrad, which corresponds to about 2-4% higher total efficiency, compared to facets of typical 1.3mrad slope error [6], a total cost reduction of 4-6% can be taken into account. Further advantages are the lower weight, the higher hail resistance and general less mirror breakage. The small possible curvature radii are important for small power plants with small towers and slant ranges in the range of 30m or below.

4. Concrete-sand foundation

For the setup of the innovative heliostat system at the site, a preformed hybrid concrete-sand foundation (Fig. 5) according to DIN 4023, EC 7 [16] has been developed. Therefore, an adequate geotechnical investigation with soil samples according to DIN 4023, EC 7, has been made: Depending on the soil conditions, earthworks have to be taken into consideration to improve the soil's stiffness and strength and to minimize its permeability. This can be achieved by compaction and/or admixing of substances. The ground improvement techniques include soil exchange, deep compaction, consolidation, injections, soil stabilization and ground freezing.

The foundation system for the heliostat consists of a block that will be additionally weighted by natural site material (sand, stones). Threaded rod anchors and nuts and an anchoring slab guarantee a perfect integration and adjustment of the overall heliostat setup. As alternative the pylon can also be embedded by concrete. Prefabricated foundations can be used for the implementation. Those parts enable a cost-effective, near-surface foundation.

Fig. 5. Prefabricated concrete ground-anchor foundation

5. Horizontal primary axis with rim drives and winch wheels

5.1. Description
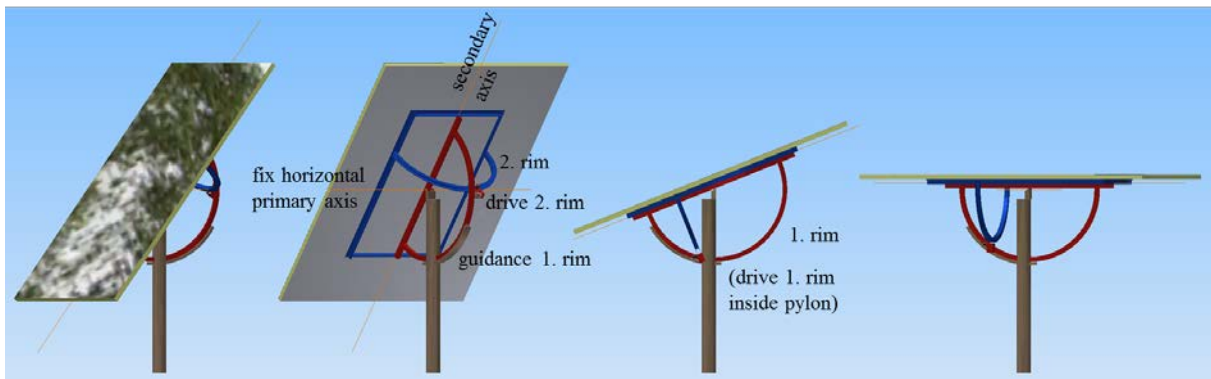
Fig. 6. Heliostat with horizontal primary axis and rim drives; red parts are pivoted only about primary axis, blue parts and sandwich panel are pivoted also about secondary axis

An illustration of a heliostat with horizontal primary axis and rim drives [17] is given by Fig. 6. The first rim can be supported by a guidance bar with sliding blocks to increase stiffness. The second rim is fixed to the mirror panel. The drive for the primary axis is mounted at the pylon, the drive for the secondary axis at the first rim. The gears can be realized by chains with bevel wheels or by winch wheels. Both rims are locked during stow. The advantages cover:

- The loads on the drives are only a fraction of the usual amount, while the back lash can be several times higher which leads to very low cost for the drives.
- Reduced loads on bearings, mirror panel, upper part of pylon and stow-position-locking devices during stow.
- Only low cost bush bearings needed.
- Higher field density and thus slightly higher field efficiency (1-2%) because of horizontal primary axis [18].
- Rims act partly as counter weights for lower energy consumption.
- No mechanical high-tech components are needed which may increase the local content.
- Higher efficiency of the complete drive train yields lower cost concerning PV cell and energy storage element (e.g. super capacitor) for autonomous operation.

The drawbacks involve:

- Extra effort for two rims, guidance bar for the first rim, sand protection for the gears (if needed) and locking devices for stow.
- Increased height of the elevation axis, which is defined by the diagonal of the mirror panel and not by the chord length as for conventional elevation-azimuth axes orientation. The increased height leads to somewhat increased wind loads, especially at the pylon base.

- Somewhat higher mounting efforts on site.
- Low stiffness for certain mirror panel orientations during operation (but, according to [5], the resulting losses in energy yield are expected to be negligible).

5.2. Winch wheels

Winch wheels fit well to the rim drive approach. On the one hand, due to the rims, one winch wheel per axis is sufficient because the both cables of each axis are running on the same circular path. Therefore, their change in length and thus their speed are the same (in opposite direction) during rotation (see Fig. 7). On the other hand, the accuracy of the rims may be low when combined with winch wheels. Further advantages of winch wheels are that they have quasi no back lash and their high efficiency.
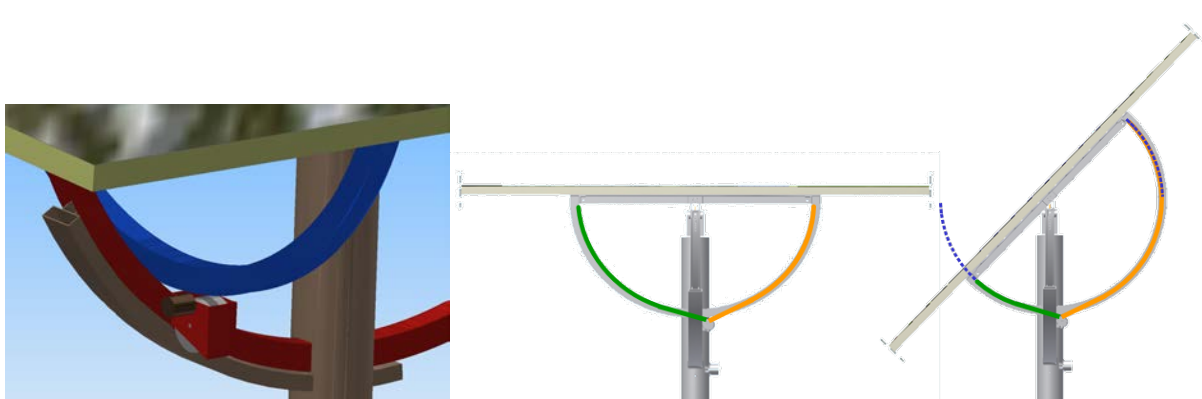

Fig. 7. Winch wheels with rims: Length change of cables of both directions during rotation is equal and thus speed when leaded on the same circular path realized by rims

5.3. Angle range limits
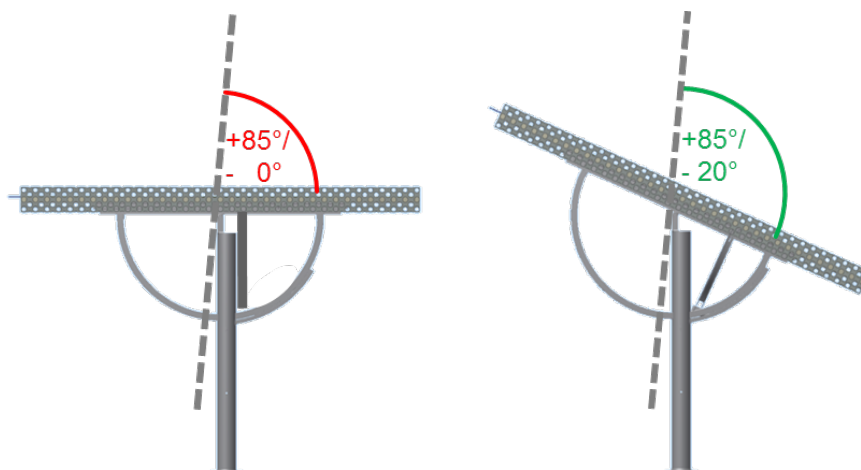
Fig. 8. Angle range limits of primary axis for central 2. rim (left) and for shifted 2. rim (right)

Regarding stiffness it would be best to place the second rim at the centre line of the mirror panel (Fig. 8, left). But, because of collision of the second rim with the pylon, the mirror could be inclined only in one direction and a limited angle range of +85°/-0° would result, with significant losses in energy especially near the tower, see Fig. 9 (all simulations performed by using subroutines of the ray tracing code MIRVAL [19], site latitude 37°, altitude 600m, without shading and blocking and 10° resolution of optimized orientation of primary axis).
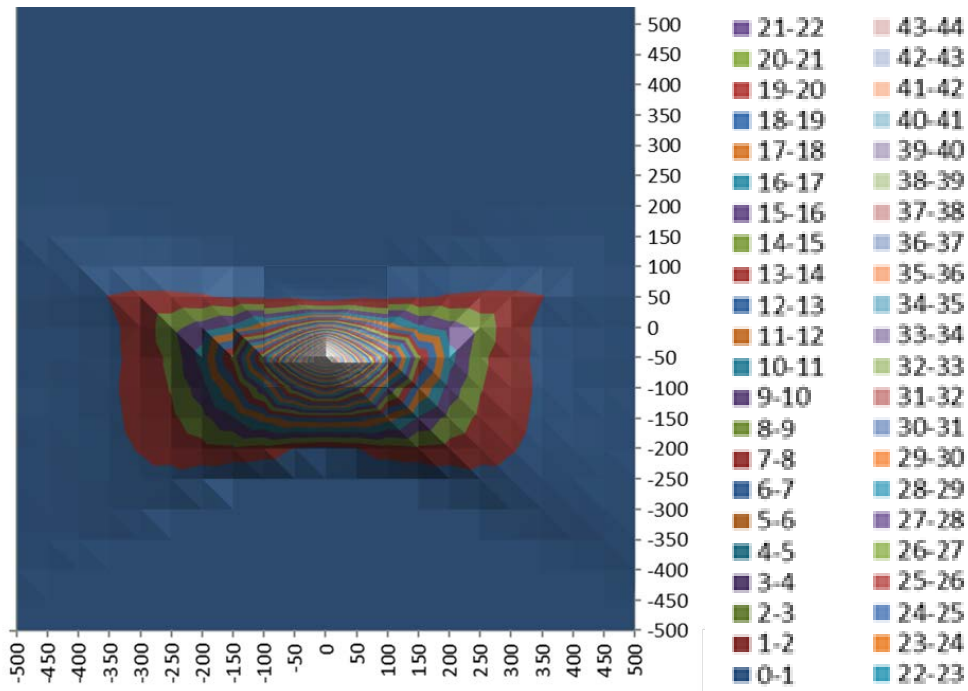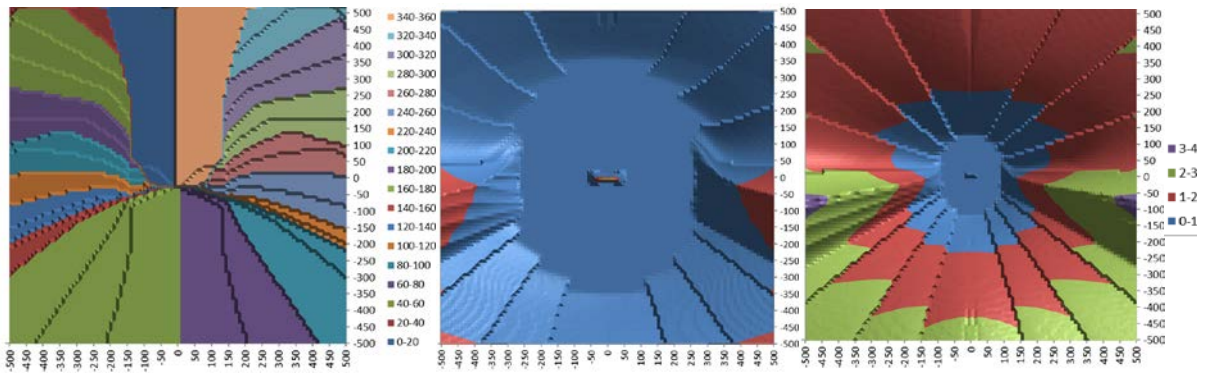
Fig. 9. Losses due to reduced angle range of primary axis (+85°/-0°) as percentage of annual energy yield, tower height 120m (position 0m/0m), optimized orientations of horizontal primary axis

If the second rim would be shifted away from the centre line to enable an angle range of +85°/-45°, all optical needed orientations could be reached. In Fig. 8, right, a compromise with an angle range of +85°/-20° is shown. The drawbacks regarding stiffness are low and the optical losses are negligible for optimized orientations of the horizontal primary axis of each heliostat (see Fig. 10).
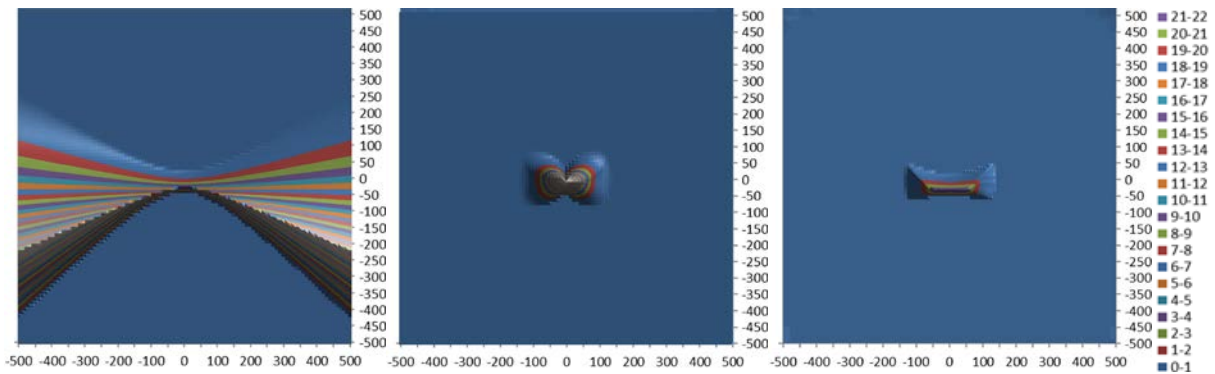
Fig. 10. Losses due to reduced angle range of primary axis (+85°/-20°) as percentage of annual yield, receiver height 120m; orientation of horizontal primary axis: east west (left), tangential to circles about tower (middle) and optimized (right)

The optimized orientations are shown in Fig. 11, left, and are close to orientations tangential to circles about the tower. Losses occur only in the south close to the tower where inclinations below -20° are needed. These low inclinations occur in the early morning and late evening hours with low DNI and high shading of the heliostats. Therefore, if the plant is in operation only for elevation of the sun higher 10°, no additional loss at all would occur. The losses near the tower reduce with the height of the tower, while they increase with the tower height at distances bigger than the accordant usual plant sizes (see Fig. 11, middle and right). For an angle range increased to +90°/-20° or for sun elevation angles higher 10° no loss at all also at the far distances for these cases would occur.

Fig. 11. Left: Optimized horizontal primary axis orientations (0°:=east, 90°:=north, receiver height 120m) Middle/Right: Losses due to reduced angle range of primary axis (+85°/-20°) as percentage of annual yield, receiver centre height 50m (middle), 20m (right), optimized orientations of horizontal primary axis

For the second axis of rotation an angle range of +70/-70 is sufficient for all heliostat positions (compare [20]).

5.4. Dimensioning

The application of FEM-tools during the design and development process of the heliostat system allows the construction of efficient and cost effective solutions. In a first step, all heliostat components have to be analysed and optimized on the individual component level. In a second step, the overall heliostat configuration has to be optimized as integral system.

The mirror facet itself has been modelled as sandwich plate with glass as upper layer, an inhomogeneous foam core and steel as backward layer. The supporting structure as well as the pylon have been modelled as standard profiles and tubes. For the simulation of the rims an unstructured mesh has been used with about 100.000 elements to evaluate rigidity and stiffness (Fig. 12).
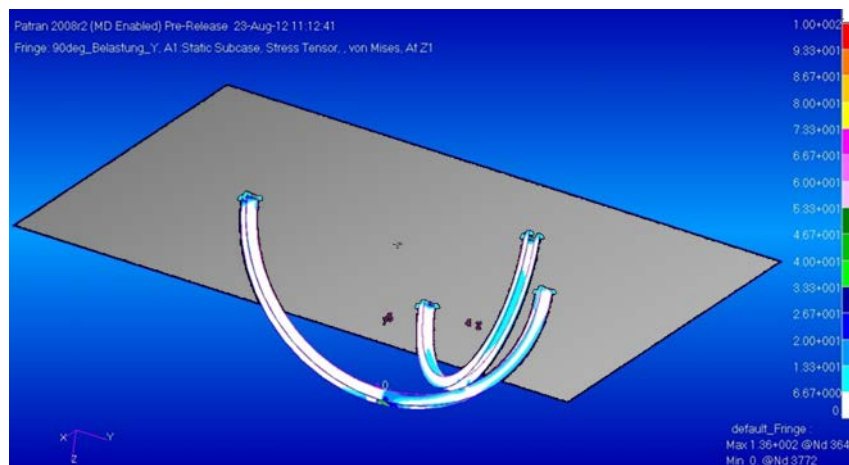
**Fig. 12. FEM-analysis of tension in rims at storm conditions**

According to the dimensioning of an 8m² heliostat, the weight of the pylon is 15kg, of the two rims 15kg, of the central bar 10kg and of the guidance bar 5kg. The (blue) L-profile frame mounted on the facet (see Fig. 6) is not needed for sufficient thickness of the sandwich facet. Overall, a weight of about 45kg for the steel structure (without mirror facet) result. Assuming steel cost of 3$/kg the cost for the steel structure is about 140$ or 18$/m².

6. Low cost motors with new commutation scheme and low cost sensors

The cost of the two additional actuators for the locking mechanism that protect the drives during stow is comparatively low, if realized using mass product components, i.e. used in automotive applications.

For the critical movement to stow position, which has to happen quite fast compared to normal tracking operation, an innovative circuitry used to drive the motor will allow to go for smaller, more cost effective stepper motors. Stepper motors are popular in heliostat drives, because they offer high precision and long lifetime at low

cost, as well as comparatively high torque at low speed. However, with standard drive electronics, the motors have to be oversized to allow for a safe operation, avoiding step-loss while overloaded, or have to be combined with self-locking gears which are in principle of low efficiency (around 40%). A new, patented commutation scheme [22] enables to operate the motors with the characteristics of a DC drive: The motors will slow down while overloaded, and speed up again when load is reduced (Fig. 13). The fact that the motors can be dimensioned without a safety margin reduces size and cost. As the method works without additional sensors, no cost is added in the drive electronics. Because no self-locking gear has to be used, the drive train is highly efficient.
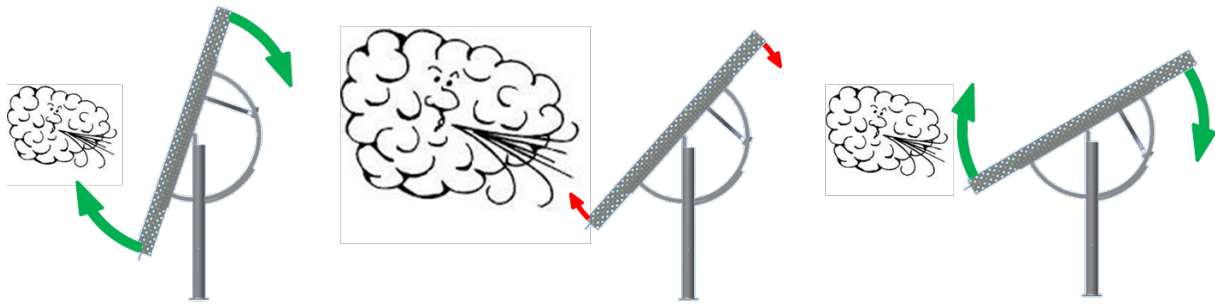
Fig. 13. Speed adaption according load to reduce motor size and to avoid self-locking gears of low efficiency

More opportunities for cost reduction but also technical challenges are to be found in the field of sensor integration. The rims are a suitable place to embed active or passive sensor targets. This enables high precision / low cost direct measurements of the angle.

7. Wireless communication and energy supply

The heliostat will be equipped with a wireless communication system based on meshed networking algorithms, as described in [8], in the meantime successfully tested and improved at the German Jülich experimental power plant. To enable autonomous operation, the unit will also be equipped with a PV panel for energy harvesting as well as with a super capacitor, serving as an energy storage device. However, the far more efficient drive train of the new heliostat design enables a significant reduction of size and, more relevant, associated cost of these two components. Savings of at least 50% are feasible.

The cost for wiring is significant, especially for (many) small heliostats, and if the local requirements demand placing it deeply in the ground. According to [1], Figure A-6, about 20% of the total cost are needed for wiring of small heliostats with 8m², while for big heliostats with 150m² mirror area about 5% are needed. Further cost reduction is achieved by the saved lightning protection: It is not necessary, because only single heliostats would be affected by a lightning strike, and not the complete field.

8. Conclusions and outlook

Summarized, the new heliostat design reflects the trend to replace heavy, inefficient structures by lightweight systems equipped with smarter electronics and more sensors. Overall, the cost goal of 120$/m² for the heliostat field can be achieved with the new heliostat concept (for high production rate and if values for overhead and profit according to [1] can be assumed). To achieve also the ambitioned cost target of 75$/m², further cost reduction can be realized, especially by new laminated mirror concepts, by optimizing the size of the heliostat and by taking new findings regarding wind load determination [14] into account. To prove the concept and the cost estimations, a prototype of 8m² shall be build.

References

[1] G.J. Kolb, S.A. Jones, M.W. Donnelly, D. Gorman, R. Thomas, R. Davenport, R. Lumia, (2007), Heliostat Cost Reduction Study, SANDIA Report SAND2007-3293.

[2] J. Gary, C. Turchi, N. Sieger, (2011). CSP and the DOE Sunshot Initiative, Proc. SolarPACES 2011 conference, Granada.

[3] A. Pfahl, (2012), Survey of Heliostat Concepts for Cost Reduction, Solar Energy Engineering, under review.

[4] A. Pfahl, M. Buselmeier, M. Zaschke, (2011), Determination of Wind Loads on Heliostats, Proc. SolarPACES 2011 conference, Granada.

[5] E. Teufel, R. Buck, A. Pfahl, G. Böing, J. Kunert, (2008), Dimensioning of Heliostat Components Under Wind and Gravity Load: the Map Approach, Proc. SolarPACES 2008 conference, Las Vegas, Nevada.

[6] C. Holze, H. Brüggen, R. Misseeuw, B. Cosijns, R. Albers, D. Isaza, R. Buck, A. Pfahl (2012), Laminated Solar Thin Glass Mirror Solution for Cost Effective CSP Systems, , Proc. SolarPACES 2012 conference, Marrakesh.

[7] C. Holze, (2011), Vorrichtung zur Optimierung des Wirkungsgrades, zum Schutz und zur Betriebsstabilisierung solarer Module bei wirkenden Umwelteinflüssen, German patent application DE10 2011 115474.8.

[8] S. Kubisch, M. Randt, R. Buck, A. Pfahl, S. Unterschütz, (2011), Wireless Heliostat and Control System for Large Self-Powered Heliostat Fields, Proc. SolarPACES 2011 conference, Granada.

[9] P. Schramek, J. Maass, (2010), High Efficient Heliostat Field Design for Solar Tower Systems, Proc. SolarPACES 2010 conference, Perpignan.

[10] T.R. Mancini, (2000), Catalog of Solar Heliostats, SolarPACES report No. III-1/00.

[11] EN 1991-1-4, (2005), Eurocode 1: Actions on Structures – Part 1-4: General Actions – Wind Actions, European Standard, Brussels.

[12] J.A. Peterka, Z. Tan, J.E. Cermak, B. Bienkiewicz, (1989). Mean and Peak Wind Loads on Heliostats. Journal of Solar Energy Engineering, 111, 158-164..

[13] J.A. Peterka, N. Hosoya, B. Bienkiewicz, J.E. Cermak, (1986). Wind Load Reduction for Heliostats, Report SERI/STR-253-2859, Solar Energy Research Institut, Golden, Colorado.

[14] D. Banks, (2011), Measuring Peak Wind Loads on Solar Power Assemblies. Proc. ICWE13, Amsterdam.

[15] B. Gong, Z. Wang, Z. Li, C. Zang, Z. Wu, (2012), Fluctuating Wind Pressure Characteristics of Heliostats, Renewable Energy 2012.

[16] Eurocode 7: Geotechnical design (EN 1997), DIN 4023: Geotechnical Investigation and Testing - Graphical presentation of logs of boreholes, trial pits, shafts and adits.

[17] A. Pfahl, (2011), Schwenkvorrichtung und Heliostat, German patent application 102011056341.

[18] T.C. Prosinečki, L. Schnatbaum, (2012), Improvements in Solar Field Layout and Molten Salt Solar Tower System Design, Proc. SolarPACES 2012 conference, Marrakesh.

[19] P.L. Leary, J.D. Hankins, (1979). A User's Guide for MIRVAL – A Computer Code For Comparing Designs of Heliostat-Receiver Optics for Central Receiver Solar Power Plants. Sandia Laboratories Report, SAND77-8280, 1979.

[20] S. Cordes, T.C. Prosinečki, K. Wieghardt, (2012), An Approach to Competitive Heliostat Fields, Proc. SolarPACES 2012 conference, Marrakesh.

[21] H. Haberstroh, T. Keck, G. Wenrebe, M. Wöhrbach, C. Husenbeth, F. von Reeken, M. Balz, (2012), Optimization of Heliostat Axes Orientations to Reduce Annual Angular Ranges, Proc. SolarPACES 2012 conference, Marrakesh.

[22] S. Moeller, E. Speck, (1997), Circuit Configuration for Affecting the Step Frequency in the Winding-Current Activation of Stepping Motor Drives with Chopped Power Output Stages, patent no. US000005959426A / DE000019609803C1.